This article was downloaded by: [University of Haifa Library]
On: 17 August 2012, At: 10:22
Publisher: Taylor & Francis
Informa Ltd Registered in England and Wales Registered Number: 1072954
Registered office: Mortimer House, 37-41 Mortimer Street, London W1T 3JH, UK

Molecular Crystals and Liquid Crystals Science and Technology. Section A. Molecular Crystals and Liquid Crystals

Publication details, including instructions for authors and subscription information:
http://www.tandfonline.com/loi/gmcl19

Structures, Ferromagnetic Ordering, Anisotropy, and Spin Reorientation for Two- and Three-Dimensional Cyano-Bridged $Mo^{3\pm}$-$Mn^{2\pm}$ Compounds

Joulia Larionova [a], Olivier Kahn [a], Stephane Golhen [b], Lahcene Ouahab [b], Rodolphe Clerac [a], Juan Bartolome [c] & Ramon Burriel [c]

[a] Laboratoire des Sciences Moléculaires, Institut de Chimie de la Matière Condensée de Bordeaux, UPR CNRS No 9048, 33608, Pessac, France

[b] Laboratoire de Chimie du Solide et Inorganique Moléculaire, UMR CNRS No 6511, Université de Rennes 1, 35042, Rennes, France

[c] Instituto de Ciencia de Materiales de Aragon, CSIC-Universidad de Zaragoza, 50009, Zaragoza, Spain

Version of record first published: 24 Sep 2006

To cite this article: Joulia Larionova, Olivier Kahn, Stephane Golhen, Lahcene Ouahab, Rodolphe Clerac, Juan Bartolome & Ramon Burriel (1999): Structures, Ferromagnetic Ordering, Anisotropy, and Spin Reorientation for Two- and Three-Dimensional Cyano-Bridged $Mo^{3\pm}$-$Mn^{2\pm}$ Compounds, Molecular Crystals and Liquid

Crystals Science and Technology. Section A. Molecular Crystals and Liquid Crystals, 334:1, 651-667

To link to this article: http://dx.doi.org/10.1080/10587259908023359

PLEASE SCROLL DOWN FOR ARTICLE

Full terms and conditions of use: http://www.tandfonline.com/page/terms-and-conditions

This article may be used for research, teaching, and private study purposes. Any substantial or systematic reproduction, redistribution, reselling, loan, sub-licensing, systematic supply, or distribution in any form to anyone is expressly forbidden.

The publisher does not give any warranty express or implied or make any representation that the contents will be complete or accurate or up to date. The accuracy of any instructions, formulae, and drug doses should be independently verified with primary sources. The publisher shall not be liable for any loss, actions, claims, proceedings, demand, or costs or damages whatsoever or howsoever caused arising directly or indirectly in connection with or arising out of the use of this material.

Downloaded by [University of Haifa Library] at 10:22 17 August 2012

Mol. Cryst. and Liq. Cryst., 1999, Vol. 334, pp. 651-667
Reprints available directly from the publisher
Photocopying permitted by license only

© 1999 OPA (Overseas Publishers Association) N.V.
Published by license under the
Gordon and Breach Science Publishers imprint.
Printed in Malaysia

Downloaded by [University of Haifa Library] at 10:22 17 August 2012

Structures, Ferromagnetic Ordering, Anisotropy, and Spin Reorientation for Two- and Three-Dimensional Cyano-Bridged Mo^{3+}-Mn^{2+} Compounds

JOULIA LARIONOVA[a], OLIVIER KAHN[a], STEPHANE GOLHEN[b], LAHCENE OUAHAB[b], RODOLPHE CLERAC[a], JUAN BARTOLOME[c] and RAMON BURRIEL[c]

[a]*Laboratoire des Sciences Moléculaires, Institut de Chimie de la Matière Condensée de Bordeaux, UPR CNRS No 9048, 33608 Pessac, France,* [b]*Laboratoire de Chimie du Solide et Inorganique Moléculaire, UMR CNRS No 6511, Université de Rennes 1, 35042 Rennes, France and* [c]*Instituto de Ciencia de Materiales de Aragon, CSIC-Universidad de Zaragoza, 50009 Zaragoza, Spain*

The compounds $K_2Mn_3(H_2O)_6[Mo(CN)_7]_2 \cdot 6H_2O$ and $Mn_2(H_2O)_5Mo(CN)_7 \cdot nH_2O$ (α phase, n = 4; β phase, n = 4.75) have been synthesized in the form of well shaped single crystals by slow diffusion of aqueous solutions containing $[Mo(CN)_7]K_2 \cdot 2H_2O$ and $[Mn(H_2O)_6](NO_3)$, respectively. The first compound has been obtained in the presence of an excess of K^+ ions. The crystal structures have been determined. $K_2Mn_3(H_2O)_6[Mo(CN)_7]_2 \cdot 6H_2O$ is two-dimensional, and $Mn_2(H_2O)_5Mo(CN)_7 \cdot nH_2O$ (α and β phases) are three-dimensional. The magnetic properties have been studied in great detail through single crystal magnetic measurements, and the magnetic phase diagrams have been determined. The three compounds exhibit a long-range ferromagnetic ordering along with a field-induced spin reorientation. Furthermore, the last two compounds show an additional magnetically ordered state which disappears when applying a sufficiently large magnetic field. The magnetic properties have been found to be dramatically modified when the non-coordinated water molecules are released. For instance, T_c is shifted from 39 to 72 K for $K_2Mn_3(H_2O)_6[Mo(CN)_7]_2 \cdot 6H_2O$, and a pronounced coercivity is observed after partial dehydration.

Downloaded by [University of Haifa Library] at 10:22 17 August 2012

INTRODUCTION

The studies concerning the Prussian-blue phases in the last few years have provided important insights on the magnetism of polymetallic compounds obtained from molecular precursors[1-17]. The rational design of high-temperature magnets, using the theoretical models developed in molecular magnetism, is one of the remarkable results of these studies[10-16]. In this respect, the high symmetry of the Prussian-blue phases was a favorable situation to monitor the magnetic properties[18-20]. As a matter of fact, the nature of the interaction between two nearest neighbor 3d magnetic ions is governed by symmetry rules involving the singly-occupied orbitals. When the symmetry of the magnetic sites is lowered, the applicability of these rules tends to vanish. The presence of 4d and 5d magnetic ions makes also these symmetry rules less heuristic, due to the strong orbital mixing through spin-orbit coupling[21]. To some extent, it is possible to say that high symmetry, 3d spin carriers, and predictable magnetic properties constitute a consistent set[22]. Conversely, low symmetry, 4d spin carriers and novel and unpredictable physical properties might constitute another consistent set. This idea led us to explore the chemistry and physics of cyano-bridged bimetallic species synthesized from the $[Mo^{III}(CN)_7]^{4-}$ precursor[23-25]. Let us remind that the Mo^{III} ion in the $[Mo(CN)_7]^{4-}$ chromophore is low-spin, with a $S_{Mo} = 1/2$ local spin[26], and that the **g**-tensor associated with the ground Kramers doublet is very anisotropic[27].

So far, we have investigated three compounds, one with a two-dimensional structure, of formula $K_2Mn_3(H_2O)_6[Mo(CN)_7]_2 \bullet 6H_2O$[25], and two with three-dimensional structures, of formula $Mn_2(H_2O)_5Mo(CN)_7 \bullet nH_2O$ (α phase, n = 4; β phase n, = 4.75)[23, 24]. Well shaped single crystals were obtained by slow diffusion of two aqueous solutions, containing

Downloaded by [University of Haifa Library] at 10:22 17 August 2012

$[Mo(CN)_7]K_2 \bullet 2H_2O$ and $[Mn(H_2O)_6](NO_3)$, respectively. The two-dimensional compound is obtained when the slow diffusion is carried out in the presence of an excess of K^+ ions. Otherwise, the slow diffusion leads to both the α and β phases of $Mn_2(H_2O)_5Mo(CN)_7 \bullet nH_2O$. This paper will present a brief overview of the results obtained so far.

THE TWO-DIMENSIONAL COMPOUND $K_2Mn_3(H_2O)_6[Mo(CN)_7]_2 \bullet 6H_2O$

Description of the Structure

The structure contains a unique Mo site along with two Mn sites, denoted as Mn1 and Mn2, as shown in Figure 1. The molybdenum atom is surrounded by two -C-N-Mn1 linkages, four -C-N-Mn2 linkages, and a terminal -C-N ligand. The symmetry of the Mo site may be viewed as a strongly distorted pentagonal bipyramid. The Mn1 site is located on a two-fold rotation axis. It is surrounded by four -N-C-Mo linkages along with two water molecules in *trans* conformation. The Mn2 site occupies a general position. It is also surrounded by four -N-C-Mo linkages and two water molecules in *trans* conformation. The geometry around both Mn1 and Mn2 may be described as a distorted octahedron.

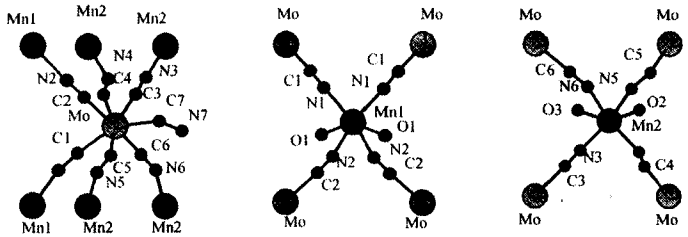

FIGURE 1 : Local structure of the molybdenum and manganese sites in $K_2Mn_3(H_2O)_6[Mo(CN)_7]_2 \bullet 6H_2O$.

The structure is two-dimensional, with anionic double-sheet layers parallel to the *bc* plane, and K^+ and non-coordinated water molecules situated between the layers, as shown in Figure 2. Each sheet is a kind of grid in the *bc* plane made of edge-sharing lozenges $[MoCNMn2NC]_2$. Two parallel sheets of a layer are connected by $Mn1(CN)_4(H_2O)_2$ units situated

between the sheets. Each $Mn1(CN)_4(H_2O)_2$ is linked through cyano bridges to four Mo atoms, two belonging to one of the sheets and two belonging to the other sheet. The thickness of a double-sheet layer is 8.042 Å, and that of the gap between two layers is 7.263 Å.

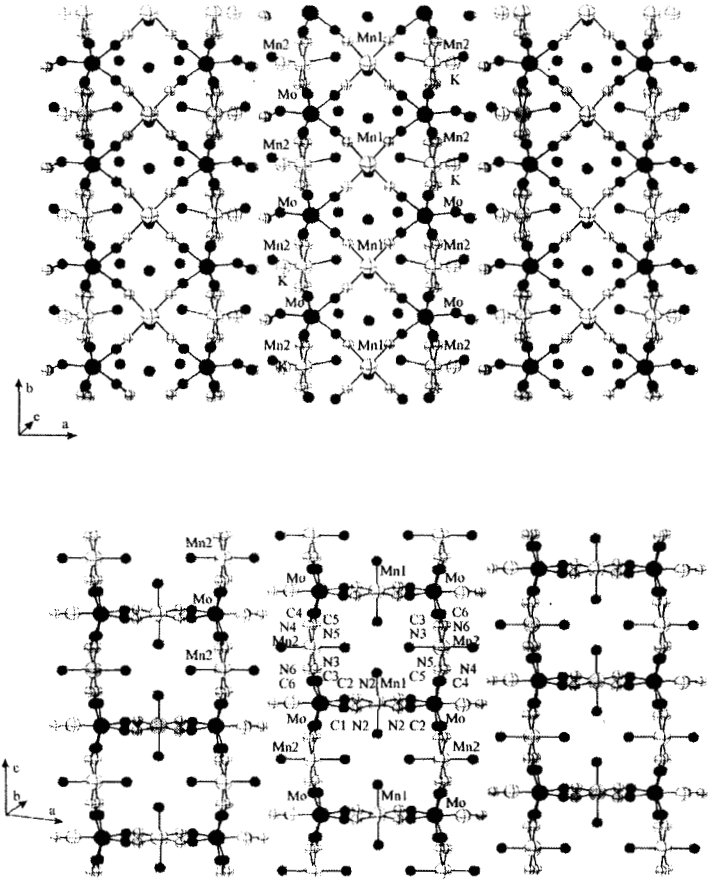

FIGURE 2 : Structure of $K_2Mn_3(H_2O)_6[Mo(CN)_7]_2 \cdot 6H_2O$ in the *ab* (top) and *ac* (bottom) planes.

Downloaded by [University of Haifa Library] at 10:22 17 August 2012

Downloaded by [University of Haifa Library] at 10:22 17 August 2012

Magnetic properties

It was first checked that the magnetic axes were collinear with the *a*, *b*, and *c** crystallographic directions by recording the angular dependences of the magnetization, M, in the *ab*, *bc**, and *ac** planes. The magnetic measurements were then carried out along these principal directions.

Figure 3 represents the temperature dependences of the magnetization along the principal axes under a magnetic field of 10 Oe. Along the three directions, *a*, *b*, and *c**, the magnetization shows a break around 39 K. The critical temperature, T_c = 39 K, may be determined accurately as the extremum of the derivative dM/dT (see the insert of Figure 3). The magnetic anisotropy of the compound is very strong. The magnetization is ten times as large along the easy magnetization axis, *b*, as along the other two directions.

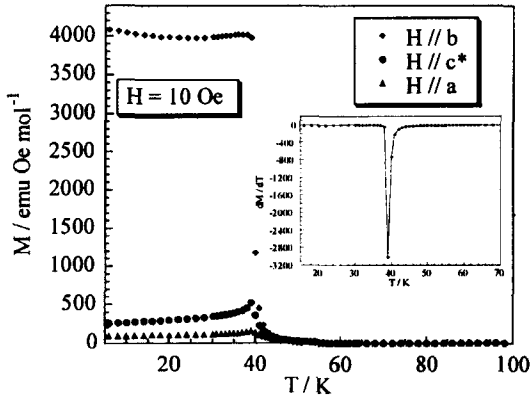

FIGURE 3 : Temperature dependences of the magnetization along the *a*, *b*, and *c** axes, under a field of 10 Oe, for $K_2Mn_3(H_2O)_6[Mo(CN)_7]_2 \bullet 6H_2O$.

Figure 4 displays the field dependences of the magnetization at 10 K along the three principal directions. Along *b*, the zero field magnetization is very high, which confirms that *b* is the easy magnetization axis, and the saturation is reached under 500 Oe. The saturation magnetization, M_{sat}, is equal to 17 Nβ, which exactly corresponds to the value expected for three S_{Mn} = 5/2 and two S_{Mo} = 1/2 spins aligned along the field direction. Along *a*, the magnetization increases progressively as the field increases, and

Downloaded by [University of Haifa Library] at 10:22 17 August 2012

reaches the saturation value above 50 kOe. The *a* axis is the hard magnetization axis. Along *c**, the differential susceptibility, dM/dH, first increases as H increases, changes of sign under 2.4 kOe (inflexion point on the M = f(H) curve), then reaches the saturation value. This behavior is characteristic of a field-induced spin reorientation[28-36]. When the field applied along *c** is weak (< 2.4 kOe), the spins remain aligned along the easy magnetization axis, *b*. When the field reaches the critical value, H_c = 2.4 Oe at 10 K, the spins progressively rotate from the *b* to the *c** axis. Finally, for a field of 3.0 K, called the saturation field, H_{sat}, the spins align along the *c** axis.

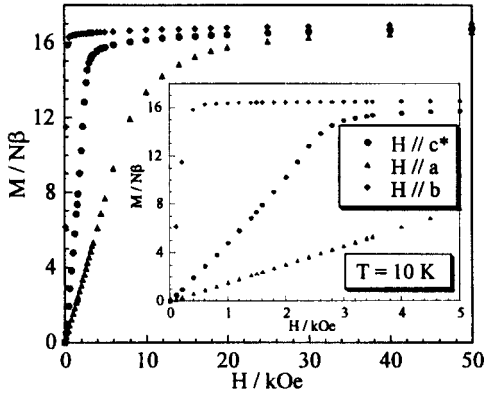

FIGURE 4 : Field dependences of the magnetization at 10 K along the *a*, *b*, and *c** axes for $K_2Mn_3(H_2O)_6[Mo(CN)_7]_2 \cdot 6H_2O$.

To establish the magnetic phase diagram, it is necessary to determine the temperature dependences of both the critical field, H_c, and the saturation field, H_{sat}[37]. For that, the field dependence of the magnetization along the *c** axis was measured every 5 K in the 5 - 40 K temperature range. The results are represented in Figure 5 (top). The critical field at each temperature was determined as the field for which the dM/dH derivative is maximum. The saturation field at each temperature was determined as the weakest field for which the M = f(H) curve is linear. The temperature dependences of H_c and H_{sat} for a field applied along the *c** axis are represented in Figure 5 (bottom).

This Figure may be viewed as the magnetic phase diagram of the compound. The H_c = f(T) and H_{sat} = f(T) curves define three domains noted I-III. Domain I corresponds to the paramagnetic domain in which the spins are either randomly oriented, or aligned along the field direction. Domain II corresponds to the ferromagnetically ordered domain in which the spins are aligned along the *b* axis. Domain III, finally, is a spin-reorientation domain in which the spins rotate from the *b* to the *c** direction as the field increases from H_c to H_{sat}.

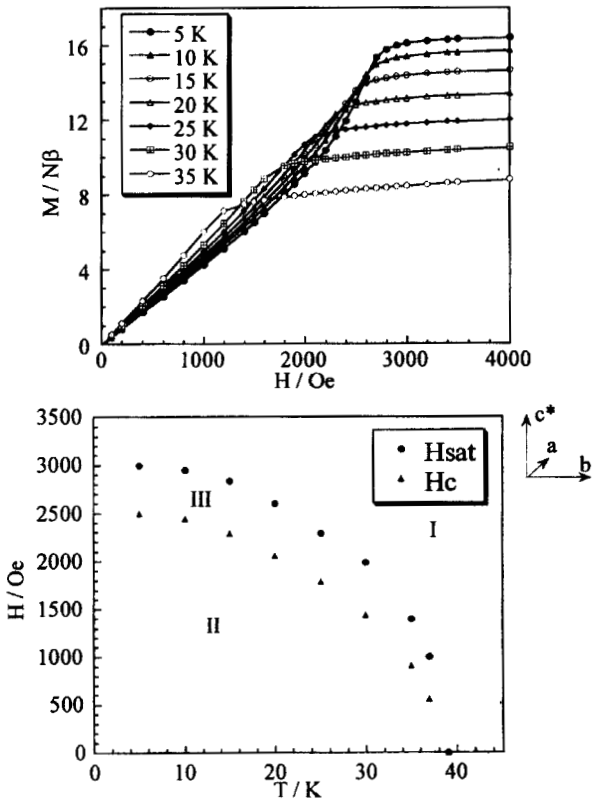

FIGURE 5 : (top) Field dependences of the magnetization measured at different temperatures along the *c** axis for $K_2Mn_3(H_2O)_6[Mo(CN)_7]_2 \bullet 6H_2O$. (bottom) Temperature dependence of the critical field, H_c, and of the saturation field, H_{sat}, for a field applied along the *c** direction.

Downloaded by [University of Haifa Library] at 10:22 17 August 2012

Downloaded by [University of Haifa Library] at 10:22 17 August 2012

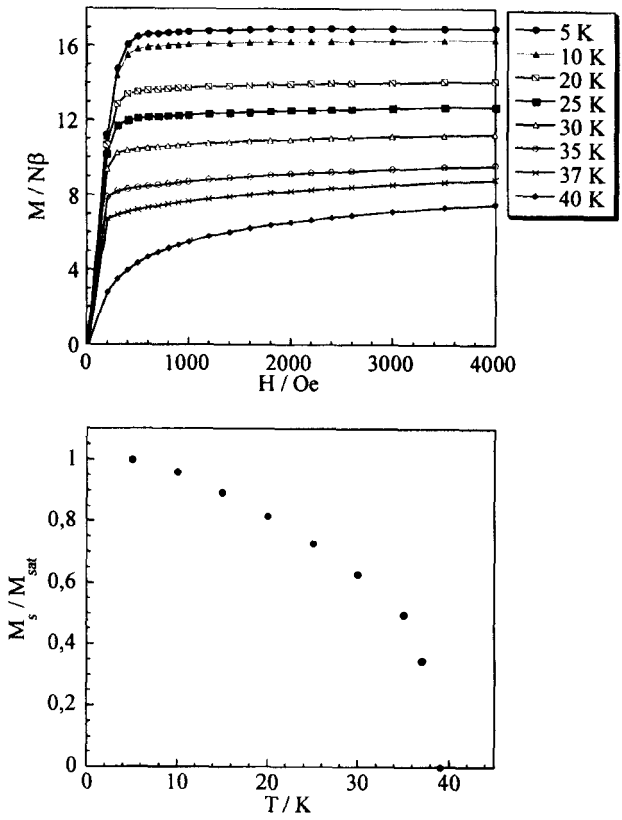

FIGURE 6 : (top) Field dependences of the magnetization along the *b* axis at different temperatures for $K_2Mn_3(H_2O)_6[Mo(CN)_7]_2 \bullet 6H_2O$. (bottom) Temperature dependence of the normalized spontaneous magnetization.

Finally, the temperature dependence of the spontaneous magnetization was determined. For that, the field dependence of the magnetization along the *b* axis was measured every 5 K. Some curves are shown in Figure 6 (top). At each temperature, the spontaneous magnetization, M_S, can be determined by extrapolating down to zero the M = f(H) data obtained in the field range where the variation is linear. The temperature dependence of the

spontaneous magnetization is represented in Figure 6 (bottom). The spontaneous magnetization vanishes at T_c = 39 K.

Modification of the Magnetic Properties through Partial Dehydration

When a single crystal of $K_2Mn_3(H_2O)_6]Mo(CN)_7]_2 \bullet 6H_2O$ is subjected to a dynamical vacuum with a primary pump for three days at room temperature, the non-coordinated water molecules are released, and the magnetic properties are deeply modified. The external shape of the crystal is not modified, which suggests that the crystallographic directions are retained. This was confirmed by measuring again the magnetization as a function of the angle between the magnetic field and the crystallographic directions of the non-dehydrated material (*ab* and *ac** planes). The temperature dependences of the magnetization were then measured along these directions. The results are represented in Figure 7. The M = f(T) curves along *b* and *c** are not distinguable. After dehydration, the *bc** plane may be considered as an easy magnetization plane, even in low field. Both in the *bc** plane and perpendicularly to this plane, the magnetization shows a break at T_c = 72 K.

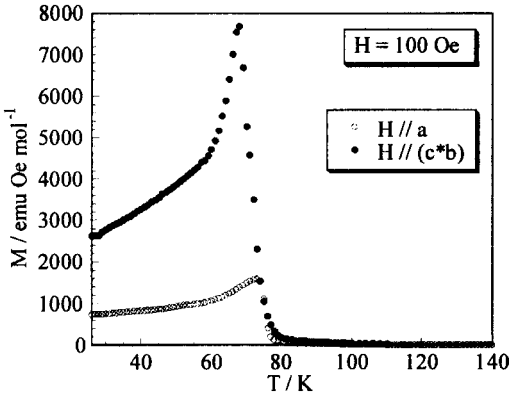

FIGURE 7 : Temperature dependences of the magnetization in the *bc* plane and along the *a* axis under 100 Oe for a partially dehydrated crystal of $K_2Mn_3(H_2O)_6[Mo(CN)_7]_2 \bullet 6H_2O$.

The field dependences of the magnetization were investigated at 10 K both in the *bc** plane and along the *a* direction. The results are displayed in

Downloaded by [University of Haifa Library] at 10:22 17 August 2012

Figure 8. In the easy magnetization plane, the saturation value of 17 Nβ corresponding to the parallel alignment of all the spins is obtained under ca. 5.0 kOe. On the other hand, along the *a* axis, the saturation is not reached yet under 50 kOe. Magnetic hysteresis are observed along both directions, with coercive fields of 1.3 kOe in the *bc** plane, and 0.55 kOe along *a*.

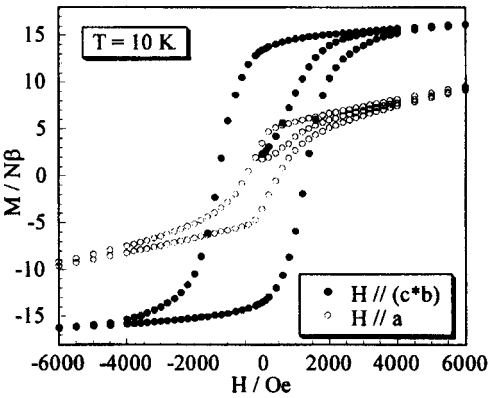

FIGURE 8 : Hysteresis loops in the *bc** plane and along the *a* axis at 10 K for a partially dehydrated crystal of $K_2Mn_3(H_2O)_6[Mo(CN)_7]_2 \bullet 6H_2O$.

THE THREE-DIMENSIONAL COMPOUNDS $Mn_2(H_2O)_3Mo(CN)_7 \bullet nH_2O$ (α AND β PHASES)

Description of the Structure of the α phase

The structure contains a unique Mo site along with two manganese sites, denoted as Mn1 and Mn2. The molybdenum atom is surrounded by seven -C-N-Mn linkages, four of them involving a Mn1 site and three of them a Mn2 site. The geometry may be described as a slightly distorted pentagonal bipyramid. Both Mn1 and Mn2 sites are in distorted octahedral surroundings. Mn1 is surrounded by four -N-C-Mo linkages and two water molecules in *cis* conformation. Mn2 is surrounded by three -N-C-Mo linkages and three water molecules in a *mer* conformation.

Downloaded by [University of Haifa Library] at 10:22 17 August 2012

Downloaded by [University of Haifa Library] at 10:22 17 August 2012

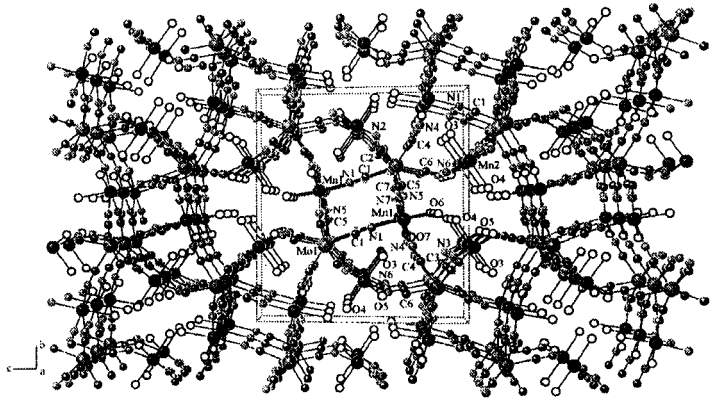

FIGURE 9 : Structure of $Mn_2(H_2O)_5Mo(CN)_7 \bullet 4H_2O$ (α phase) viewed along the *a* direction.

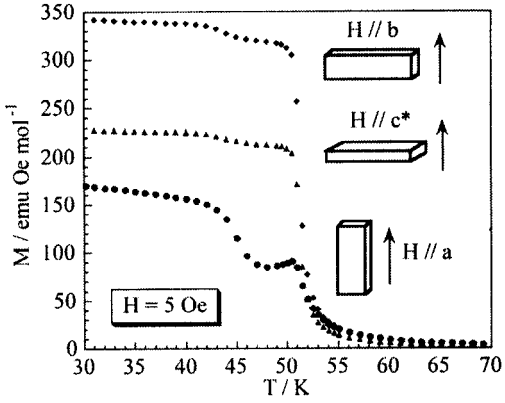

FIGURE 10 : Temperature dependences of the magnetization along the *a*, *b* and *c** directions, under an external field of 5 Oe, for $Mn_2(H_2O)_5Mo(CN)_7 \bullet 4H_2O$ (α phase).

The three-dimensional organization may be described as follows : Edge-sharing lozenge motifs $(MoCNMn1NC)_2$ form bent ladders running along the *a* direction. Each ladder is linked to four other ladders of the same kind along the [011] and [01-1] directions through cyano bridges. These

ladders are further connected by the $Mn2(CN)_3(H_2O)_3$ groups. Mn2 is linked to a Mo site of one of the ladders and to two Mo sites of the adjacent ladder. The structure as a whole viewed along the *a* direction is represented in Figure 9.

Magnetic Properties of the α phase

All the magnetic measurements were carried out on single crystals with the external field applied along the *a*, *b*, and *c** directions, which were checked to be the magnetic axes.

The temperature dependences of the magnetization, M, along the three crystallographic directions under a field of 5 Oe are represented in Figure 10. The three curves exhibit a break with an inflexion point at T_c = 51 K, characteristic of a long-range ordering, and another transition at T_c' = 43 K. Moreover, Figure 10 shows that the *b* direction is the easy magnetization direction in zero or low field.

The onset of a long range ferromagnetic ordering at 51 K was confirmed by the temperature dependence of the heat capacity shown in Figure 11. The heat capacity exhibits a characteristic lambda peak at the critical temperature.

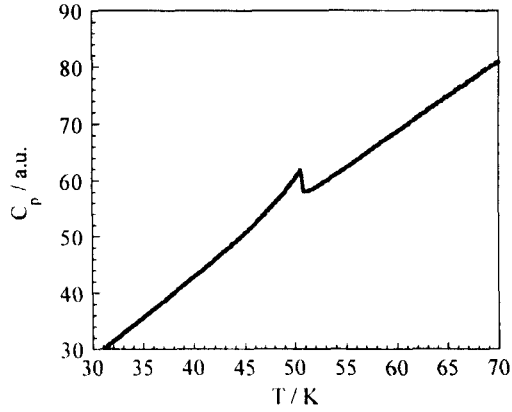

FIGURE 11 : Temperature dependence of the heat capacity for $Mn_2(H_2O)_5Mo(CN)_7 \bullet 4H_2O$ (α phase).

Downloaded by [University of Haifa Library] at 10:22 17 August 2012

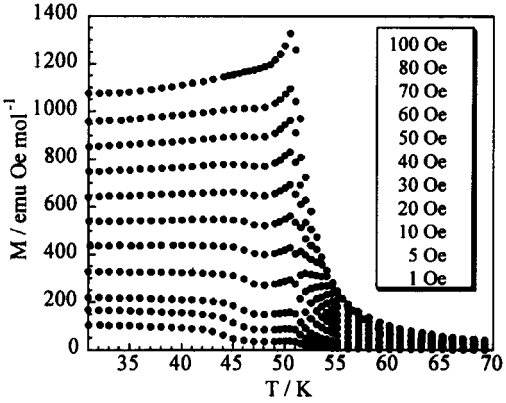

FIGURE 12 : Temperature dependences of the magnetization along the *a* direction, using different values of the external field, for $Mn_2(H_2O)_5Mo(CN)_7 \bullet 4H_2O$ (α phase).

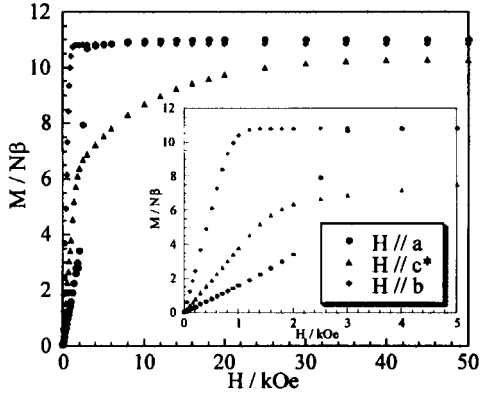

FIGURE 13 : Field dependences of the magnetization at 5 K along the *a*, *b*, and *c** directions for $Mn_2(H_2O)_5Mo(CN)_7 \bullet 4H_2O$ (α phase).

In order to obtain more insights on the magnetic anomaly detected at 43 K, visible essentially along the *a* direction, the magnetization along this direction was measured with an external field varying from 1 up to 100 Oe. The results are displayed in Figure 12. T'_c is shifted toward higher temperatures as the magnetic field increases, and eventually, for a field of

Downloaded by [University of Haifa Library] at 10:22 17 August 2012

Downloaded by [University of Haifa Library] at 10:22 17 August 2012

ca. 100 Oe, merges with the transition at 51 K. For each field the transition temperature, T'_c, was determined as the inflexion point of the M = f(T) curve.

Figure 13 represents the field dependences of the magnetization at 5 K along the *a*, *b*, and *c** directions. These curves are strictly identical when increasing and decreasing the field; the compound exhibits no coercivity. Along the easy magnetization direction, *b*, the saturation is reached with ca. 1 kOe. The saturation magnetization is found equal to 11 Nβ. This value corresponds exactly to what is expected for the S_{Mo} = 1/2 and S_{Mn} = 5/2 local spins aligned along this direction. Along the *c** direction, the magnetization increases progressively when applying the field, and even at 50 kOe the saturation is not totally reached. Along the *a* direction, the M versus H curve reveals again a field-induced spin reorientation, with a rotation of the spins between the critical field, H_c, and the saturation field, H_{sat}. The temperature dependences of H_c and H_{sat} were determined, as explained in the case of the two-dimensional compound. The H_c and H_{sat} = f(T) curves are shown in the magnetic phase diagram of Figure 14. This diagram is more complex than that of the previous compound. It presents four domains. Domain I is the paramagnetic domain. Domain II is a ferromagnetic domain in which the spins are essentially aligned along the *b* direction. Domain III is limited to the 43 - 51 K temperature range and a field along *a* lower than 100 Oe. It is another ferromagnetically ordered domain. Domain IV, finally, is limited by the H_c = f(T) and H_{sat} = f(T) curves, and corresponds to a mixed domain in which the spins may rotate from the *b* to the *a* direction. It is difficult to specify the differences between the two magnetically ordered domains II and III. Assuming that the magnetic symmetry decreases as the temperature is lowered, one may assume that domain III is a strictly ferromagnetic domain, and that domain II is a canted ferromagnetic domain, with a component of the magnetic moment along the *a* direction. Only polarized neutron diffraction data could allow us to determine unambiguously the nature of the two domains.

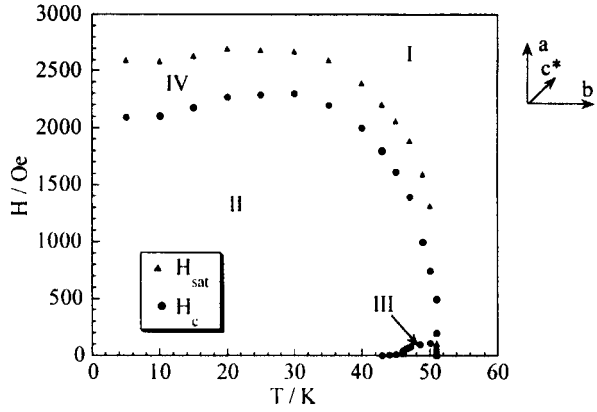

Figure 14 : Magnetic phase diagram for $Mn_2(H_2O)_5Mo(CN)_7 \bullet 4H_2O$ (α phase); the full lines are just eye-guides (see text).

The temperature dependence of the spontaneous magnetization was also determined for this compound.

The structure of the β phase is shown in Figure 15. The local environments of the metal sites are the same as for the α phase, but the three-dimensional organization is different. Each ladder made of edge-sharing lozenge motifs is surrounded only by two instead of four identical ladders. This phase again exhibits a ferromagnetic transition at 51 K. It is even more anisotropic than the α phase, and the magnetic phase diagram is even more complex.

The partial dehydration of the α or β phase leads to the same compound which exhibits a long-range ferromagnetic ordering at 66 K along with a coercive field of 850 Oe at 5 K.

CONCLUSION

A new family of cyano-bridged bimetallic compounds has been discovered, whose richness in terms of both structures and physical properties is exceptional. The compounds of this family possess a remarkable capability to grow as well-shaped single crystals, and the physical studies performed on these single crystals reveal many peculiarities. Not only, the compounds are

Downloaded by [University of Haifa Library] at 10:22 17 August 2012

genuine ferromagnets, but they exhibit many interesting features in addition to the ferromagnetic ordering, such as the presence of several magnetically ordered phases (for the α and β phases of $Mn_2(H_2O)_5Mo(CN)_7 \bullet nH_2O$) and spin reorientations. To the best of our knowledge, these features have not been investigated so far in the field of molecular magnetism. A key role in this interesting physics is played by the extremely strong anisotropy of the compounds. This anisotropy has two origins, namely the structural anisotropy, and the local anisotropy of the low-spin Mo^{III} ion.

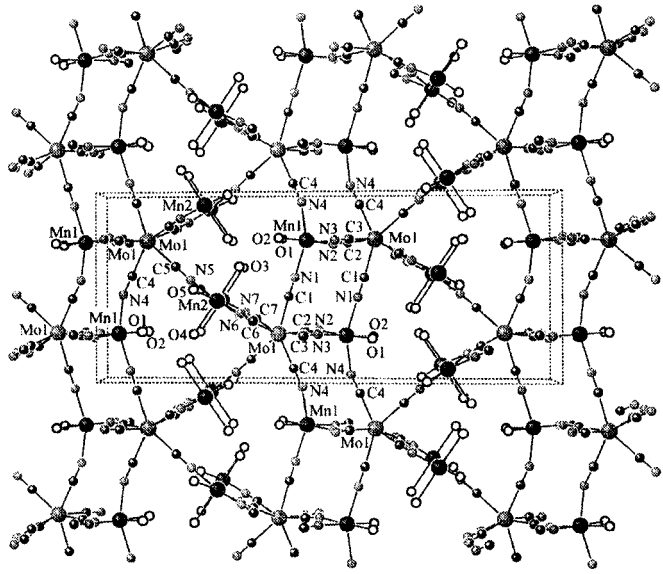

FIGURE 15 : Structure of $Mn_2(H_2O)_5Mo(CN)_7 \bullet 4.75H_2O$ (β phase) viewed along the *a* direction.

Acknowledgements

This work was partly funded by the TMR Research Network ERB 4061 PL-97-0197 of the European Union, entitled : Molecular Magnetism; from Materials toward Devices.

Downloaded by [University of Haifa Library] at 10:22 17 August 2012

Downloaded by [University of Haifa Library] at 10:22 17 August 2012

References

[1] R. M. Bozorth, H. J. Williams, D. E. Walsh, *Phys. Rev.* **103,** 572 (1956).

[2] A. N. Holden, B. T. Matthias, P. W. Anderson, H. W. Lewis, *Phys. Rev.* **102,** 1463 (1956).

[3] F. Herren, P. Fischer, A. Ludi, W. Hälg, *Inorg. Chem.* **19,** 956 (1980).

[4] A. Ludi, H. U. Güdel, *Struct. Bonding(Berlin)* **14,** 1 (1973).

[5] R. Klenze. B. Kanellakopoulos, G. Trageser, H. Eysel, *J. Chem. Phys.* **72,** 5819 (1980).

[6] W. D. Griebler, D. Babel, *Z. Naturforsch. B* **37,** 832 (1982).

[7] D. Babel, *Comments Inorg. Chem.* **5,** 285 (1986).

[8] D. Babel, W. Kurtz, in *Solid State Chemistry 1982,* R. Metselaar, H. J. M. Heijligers, J. Schoonman, Eds.; Elsevier, Amsterdam, 1983.

[9] W. Kurtz, D. Babel, *Solid State Commun.* **48,** 277 (1983).

[10] V. Gadet, T. Mallah, I. Castro, M. Verdaguer, *J. Am. Chem. Soc.* **114,** 9213 (1992).

[11] T. Mallah, S. Thiébaut, M. Verdaguer, P. Veillet, *Science* **262,** 1554 (1993).

[12] T. Mallah, S. Ferlay, C. Auberger, C. Helary, F. L'Hermite, R. Ouahès, J. Vassermann, M. Verdaguer, P. Veillet, *Mol.Cryst. Liq. Cryst.* **273,** 141 (1994).

[13] S. Ferlay, T. Mallah, R. Ouahès, P. Veillet, M. Verdaguer, *Nature* **378,** 701 (1995).

[14] W. R. Entley, C. R. Treadway, G. S. Girolami, *Mol.Cryst. Liq. Cryst.* **273,** 153 (1994).

[15] W. R. Entley, G. S. Girolami, *Science* **268,** 397 (1995).

[16] W. R. Entley, G. S. Girolami, *Inorg.Chem.* **33,** 5165 (1994).

[17] O. Sato, T. Iyoda, A. Fujishima, K. Hashimoto, *Science* **272,** 704 (1996).

[18] O. Kahn, *Adv. Inorg. Chem.* **43,** 179 (1995).

[19] O. Kahn, *Nature* **378,** 667 (1995).

[20.] O. Kahn, *Molecular Magnetism,* VCH, New York, 1993.

[21] J. Larionova, B. Mombelli, J. Sanchiz, O. Kahn, *Inorg. Chem.* **37,**679 (1998).

[22] O. Kahn, *Angew. Chem. Int. Ed. Engl.* **24,** 834 (1985).

[23] J. Larionova, J. Sanchiz, S. Golhen, L. Ouahab, O. Kahn, O.J. *Chem. Soc., Chem. Commun.* 953 (1998).

[24] J. Larionova, R. Clerac, J. Sanchiz, O. Kahn, S. Golhen, L. Ouahab, *J. Am. Chem. Soc.* In press.

[25] J. Larionova, O. Kahn, S. Golhen, L. Ouahab, R. Clerac, submitted to *Inorg. Chem.*

[26] G.R. Rossman, F.D. Tsay, H.B. Gray, *Inorg. Chem.* **12,** 824 (1973).

[27] M.B. Hursthouse, K.M.A. Maijk, A.M. Soares, J.F. Gibson, W. P. Griffith, *Inorg. Chim. Acta* **45,** L81 (1980).

[28] E. Stryjewski, N. Giordano, *Adv. Phys.* **26,** 487 (1977).

[29] D. Givord, H.S. Li, R. Perrier de la Bathie, *Solid State Commun.* **51,**857 (1984).

[30] S. Hirosawa, Y. Matsuura, H. Yamamoto, S. Fujimura, M. Sagawa, H.Yamauchi, *J. Appl. Phys.* **59,** 873 (1986).

[31] M.A. Salgueiro da Siva, J.M. Moreira, J.A. Mendes, V.S. Amaral, J.B. Sousa, S.B. Palmer, *J, Phys. : Condens. Mater.* **7,** 9853 (1995).

[32] P.C. Canfield, B.K. Cho, K.W. Dennis, *Physica B* **215,** 337 (1995).

[33] B. Garcia-Landa, E. Tomey, D. Fruchart, D. Gignoux, R. Skolozdra, *J. Magn. Magn. Mater.* **157–158,** 21 (1996)).

[34] W.A. Mendoza, S.A. Shaheen, *J. Appl. Phys.* **79,** 6327 (1996).

[35] G. Cao, S. McCall, J.E. Crow, *Phys. Rev. B* **55,** R672 (1997).

[36] X.C. Kou, M. Dahlgren, R. Grössinger, G. Wiesinger, *J. Appl. Phys.* **81,** 4428 (1997).

[37] Herpin, A. *Théorie du magnétisme,* Presses Universitaires de France : Paris, 1968.